

Characterization of Epoxidized Natural Rubber/Ethylene Vinyl Acetate (ENR-50/EVA) Blend: Effect of Blend Ratio

Zurina Mohamad,¹ H. Ismail,¹ R. Chantara Thevy²

¹*Division of Polymer, School of Materials and Mineral Resources Engineering, USM, 14300 Seri Ampangan, Seberang Perai Selatan, Malaysia*

²*Malaysian Institute for Nuclear Technology Research (MINT), Bangi, 43000 Kajang, Malaysia*

Received 31 January 2005; accepted 29 April 2005

DOI 10.1002/app.22154

Published online in Wiley InterScience (www.interscience.wiley.com).

ABSTRACT: Epoxidized natural rubber/Ethylene vinyl acetate copolymer (ENR-50/EVA) blends with different ratios were prepared by using a Haake internal mixer. The effect of the blend ratio on the processing, tensile properties (such as tensile strength, elongation at break, Young's modulus and stress-strain behavior), morphology, dynamic mechanical properties, and thermal properties has been investigated. The tensile properties increase with the increase of EVA content, whereas the stabilization torque increases with the increase of ENR-50 content in the blend. In 40:60 and 50:50 blend of ENR-50/EVA, both the phases exist as con-

tinuous phases, producing a co-continuous morphology. At these blend ratio, the drastic change in properties were noted, indicating that the phase inversion occurs. The results on dynamic mechanical properties revealed that the blends are compatible. Blending of ENR-50 and EVA lead to the improvement in thermal stability and 50:50 blend ratios is the most stable blend. © 2005 Wiley Periodicals, Inc. *J Appl Polym Sci* 99: 1504–1515, 2006

Key words: ENR-50; EVA; TPE; Blend ratio

INTRODUCTION

Polymer blending was recognized in the last few decades as a most promising way to prepare new material with tailored individual properties. Blending of existing commodity or engineering polymers often can be implemented more rapidly and it is less expensive than realization of new polymer chemistry, including development of monomer synthesis and polymerization technology. Extensive studies have been carried out in the area of polymer blend. This study included rubber-rubber blend,^{1–4} rubber-plastic blend^{5–8}, and plastic-plastic blend.^{9–12}

Epoxidized natural rubber (ENR) is a chemically modified natural rubber (NR). The epoxidation of NR to produce ENR involves the random introduction of epoxide groups onto the double bond of the NR polymer chain. ENR poses excellent properties such as oil resistance, gas impermeability, good wet grip, and high damping characteristics.¹³ The oil resistance of ENR-50 is due to the polarity of the epoxide group. The resistant to hydrocarbons of NR found to be improved with the increase in epoxidation level. However the resistance to polar solvent shows a decline

with the epoxide content in NR.¹⁴ Currently Malaysian Rubber Board produces ENR with the trade name Epoxyprene. Two grades are available, namely ENR 25 and ENR 50, with 25, and 50 mol % epoxidation, respectively. However the market and applications for ENR found to be limited. Thus attempts are being made to diversify the usage and application of this rubber, especially in advanced engineering field. As mention earlier, blending with other polymer is the easiest and the cheapest way to tailor the properties of ENR and at the same time reduce the material cost. Furthermore, the presence of oxirane group in ENR was found to be effective in causing specific interaction with a second polymer.¹⁵

Ethylene vinyl acetate copolymers (EVA) are randomly structured polymers, which offer excellent ozone resistance, weather resistance, and excellent mechanical properties.¹⁶ EVA is chosen to be blended with ENR-50 because of its excellence properties and halogen-free thermoplasticity. It is hoped that the blends of EVA and ENR will lead to the production of halogen-free materials, which may suit many applications that are currently dominated by PVC.

EXPERIMENTAL

Materials

Epoxidized natural rubber, ENR 50, with 50 mol % epoxidation (grade EPOXYPRENE 50) used in this

Correspondence to: Z. Mohamad (r-zurina@utm.my).

study was obtained from Kumpulan Guthrie Sdn. Bhd., Malaysia with specific gravity value of 1.03. Ethylene vinyl acetate (Grade H2020) having 15% vinyl acetate content with MFI value of 1.5 g/10 min and density of 0.93 g/cm³ was purchased from The Polyolefin Company, Singapore.

Mixing procedure

The ENR-50/EVA blends were prepared by melt-mixing the ENR-50 and EVA in a Haake Rheomix Polydrive R 600/610 at 120°C and rotor speed at 50 rpm for 6 min. The blend ratios of ENR-50/EVA used in this studies are 0/100, 20/80, 40/60, 50/50, 60/40, 80/20, and 100/0 (wt %). EVA was charged into the mixing chamber and allowed to melt for 2 min. Then ENR-50 was added to the molten EVA and the mixing was continued for a further 4 min. A torque versus time curve was plotted for each composition during mixing process to monitor processing condition. The samples were then compression molded at 120°C for 5 min and cooled for 2 min to produce 1 and 2 mm thick sheets.

Tensile properties

The tensile properties were measured with a Tensometric tensometer M 500 according to ASTM D 412 at 50 mm/min crosshead speed. The molded samples of 1 mm thickness were cut into standard test pieces using a Wallace die cutter.

Morphology study

Examination of the fractured surfaces was performed using a scanning electron microscope (SEM; Leica Cambridge S-360 model). The samples were cryogenically fractured and the surface was treated with methyl ethyl ketone to selectively etch the ENR-50 phase. All samples were examined after first sputter coating with gold to avoid electrostatic charging and poor image resolution.

Dynamic mechanical analyzer

Dynamic mechanical properties were measured with PerkinElmer dynamic mechanical analyzer DMA 7e. The experiment was conducted in a 3 point bending mode at a frequency of 1 Hz. The temperature was increased at 5°C/min over the range of -70 to 30°C. The dimensions of the samples were approximately 2 mm thick, 15 mm length, and 10 mm width.

Differential scanning calorimetry (DSC)

Differential scanning calorimetry (DSC) thermograms were obtained with a PerkinElmer DSC-7 at a heating rate of 20°C/min. The samples were scanned from 30

to 160°C using nitrogen air. The melting temperature (T_m) and the heat of fusion (ΔH_f) were measured during the heating cycle.

Thermogravimetric analysis

The thermogravimetry and derivative thermogravimetry were carried out in a PerkinElmer Pyrist 6 TGA analyzer. The samples were scanned from 30 to 600°C at a heating rate of 20°C/min.

Density

Density of all samples was measured at room temperature in purified helium using gas pycnometer (AccuPyc 1330 model; Micromeritics).

RESULTS AND DISCUSSION

Processing (torque development)

The torque–time curves were used to present the processibility of the blends.¹⁷ Figure 1 shows the torque–time curves of ENR-50/EVA blend at different blend ratios. In general all curves have two peaks (A and B), representing the loading peak of EVA and ENR-50, respectively, except the curve for pure EVA. The torque sharply increases as EVA was charged into the mixing chamber and gradually decreases and stable at about 2 min as EVA undergo fusion process. Again the torque shows the similar trend as ENR-50 was loaded at 2nd minute and stable at about 6th minute of mixing. The maximum torque for ENR-50 is higher than that for EVA because of the higher viscosity of ENR-50, thus giving higher resistance to the rotor speed. Figure 1 shows that the first peak increases as the EVA content increases and the second peak shows similar trend as ENR-50 content increases. The effect of blend ratio on the stabilization torque at 6th minute was shown in Figure 2. As can be seen, the stabilization torque increases with the increase of ENR-50 content in the blend. This is due to the higher viscosity of ENR-50 when compared to EVA.

Tensile properties

Figures 3, 4 and 5 show the tensile properties of the ENR-50/EVA blend at different blend ratios. Stress–strain curves of the samples are shown in Figure 3. The curves represent the difference in deformation characteristics of pure polymer and blend under an applied stress. Pure EVA and EVA dominant blends show higher initial modulus with a yield point. At higher strains, these blends show a gradual increase in stress. Such an observation could be due to the orientation of the polyethylene crystalline hard segments of EVA in the continuous phase at the direction of ap-

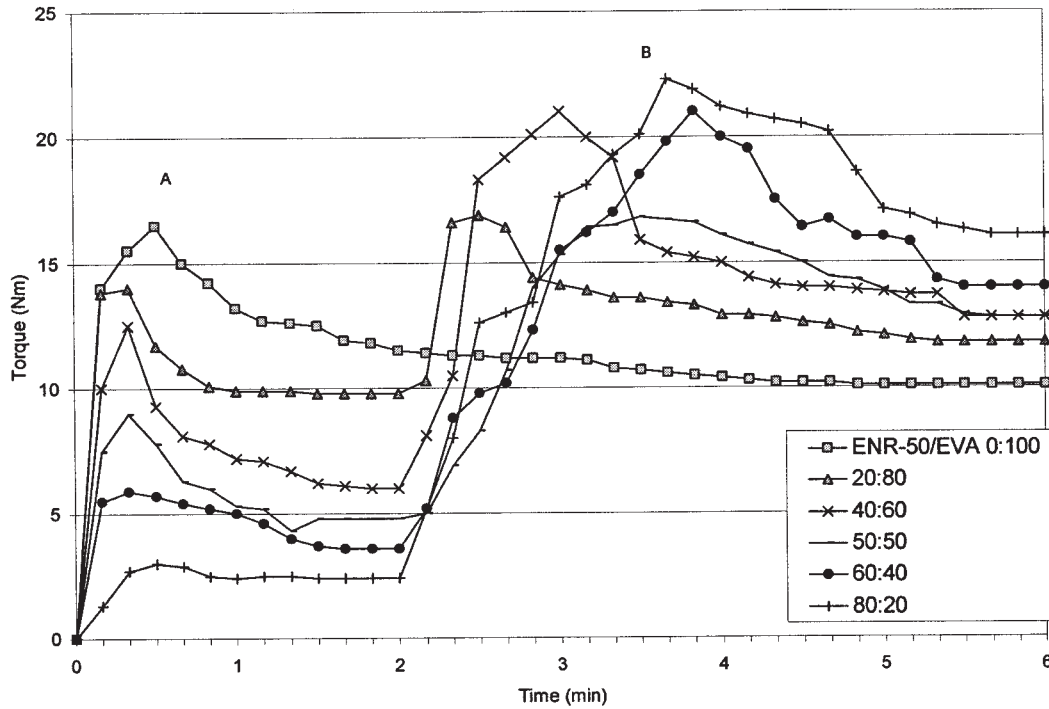


Figure 1 Torque-time curves of ENR-50/EVA blend at different blend ratios.

plied stress. These blends also show the elastic and inelastic region, in which the samples undergo yielding, and the strain induces crystallization in the inelastic region. ENR-50/EVA with 50:50 blend ratios with a co-continuous morphology shows a stress-strain behavior, which is intermediate between those of the

other blend ratios. Varghese et al.⁵ reported similar findings on nitrile rubber/ethylene vinyl acetate blend.

Tensile strength, Young's modulus, and elongation at break increase with the increase of EVA content (Figs. 4 and 5). These properties increase sharply when

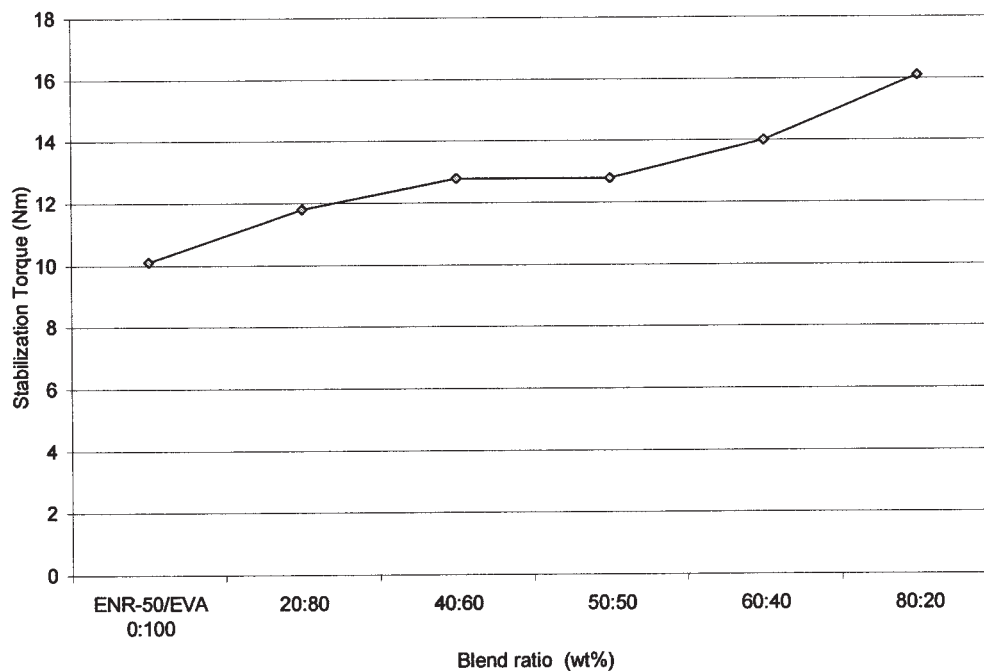


Figure 2 Stabilization torque at the end of mixing time (6 min) of ENR-50/EVA blend at different blend ratios.

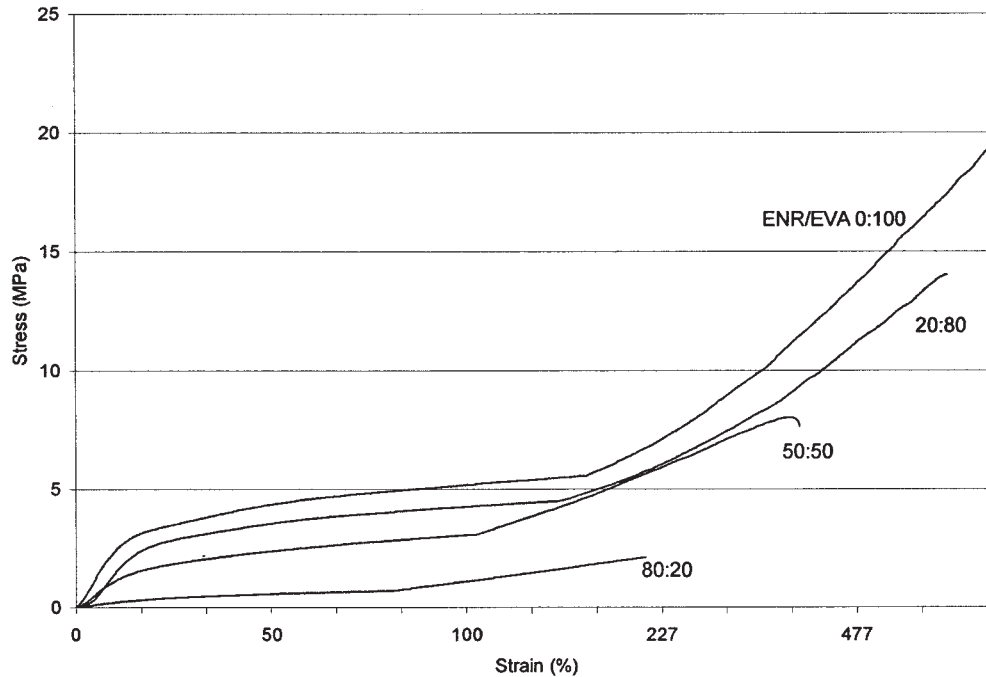


Figure 3 Stress-strain curves of ENR-50/EVA blend at different blend ratios.

the EVA content is more than 60 wt %. This is due to the fact that at 60 wt % and more EVA content, it becomes the continuous phase as evident from the SEM study.

Morphology of the blend

The major factors that affect the blend morphology are volume fraction and viscosity. Continuity of the

phase is favored by high volume fraction and low viscosity.⁵ The SEM micrographs of ENR-50/EVA blends are shown in Figure 6. In ENR-50/EVA blend with 20:80 and 40:60, ENR-50 is dispersed in the EVA matrix, whereas in ENR-50/EVA with 50:50, 60:40, and 80:20 both the phases exist as continuous phases, producing a co-continuous morphology.

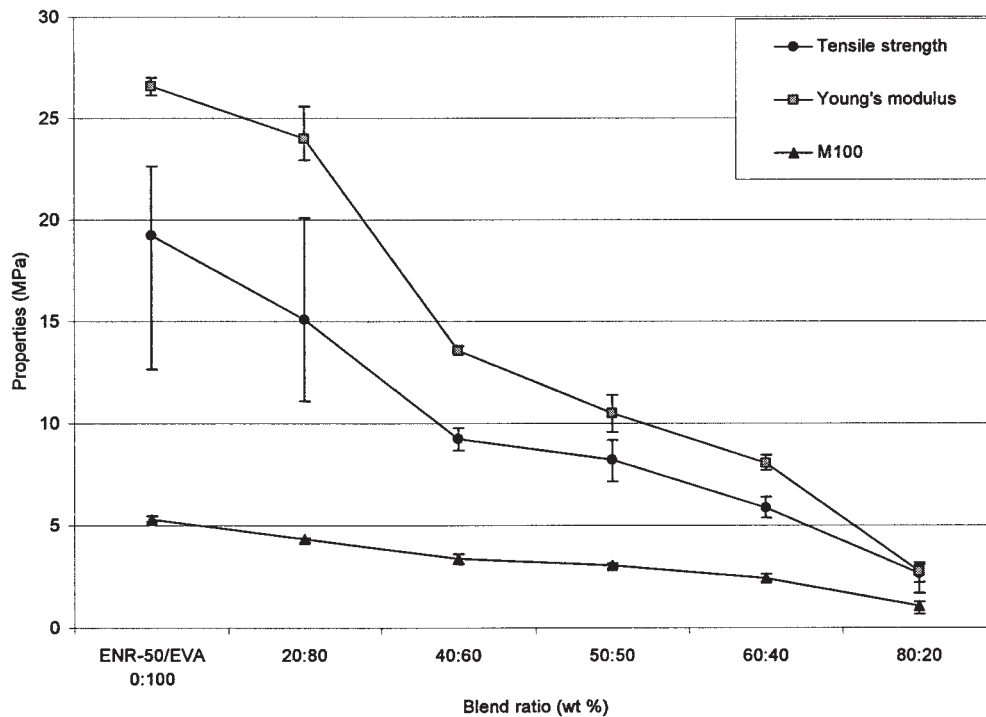


Figure 4 The effect of blend ratio on the tensile strength and Young's modulus of ENR-50/EVA blend.

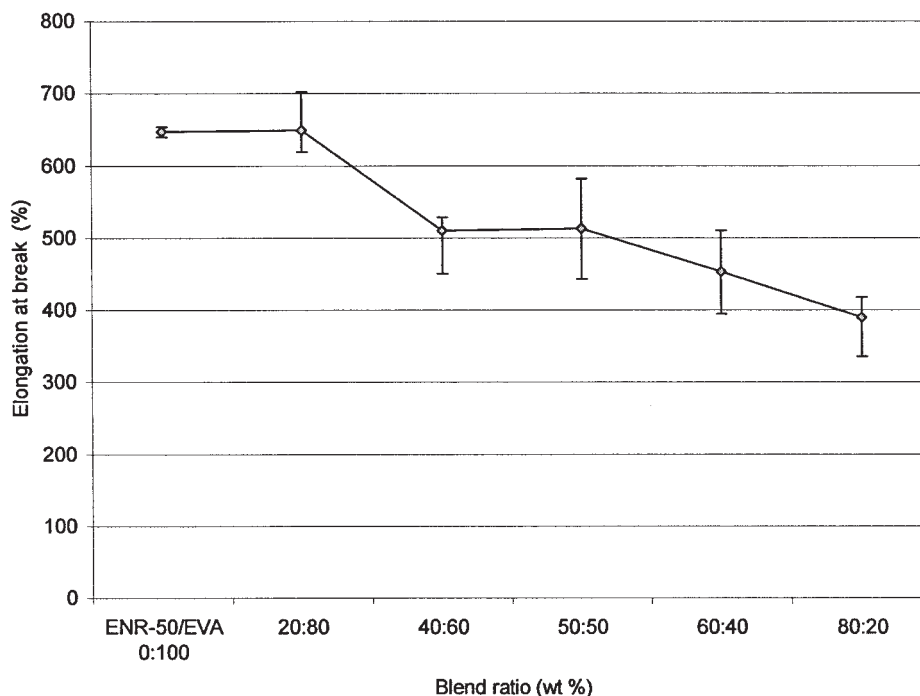


Figure 5 The effect of blend ratio on the elongation at break of ENR-50/EVA blend.

Dynamic mechanical analysis

The dynamic mechanical properties of epoxidized natural rubber/ethylene vinyl acetate (ENR-50/EVA) blends are listed in Table I. The influence of the storage modulus (E') and loss modulus (E'') with the temperature for the blends at different blend ratios are shown in Figures 7 and 8. The storage modulus curves present three distinct regions, namely glass region, transition region, and rubbery region. Pure ENR-50 shows a higher storage modulus at lower temperature. Above the glass transition temperature, ENR-50 changes sharply from glassy state to amorphous state. As EVA content in the blends increases, the transition becomes not so sharp because of the influence of the crystalline part of the EVA phase.¹⁸ This is because in crystalline materials, during the transition, only the amorphous part undergoes segmental motion, whereas the crystalline region remains a crystalline solid until reaching the temperature of melting. The storage modulus slightly increases after transition region upon increasing of the EVA content in the blend. This indicates that at temperature higher than transition region, the blend material become more rigid as the EVA content increases, hence the increase in the ability of the materials to resist deformation.

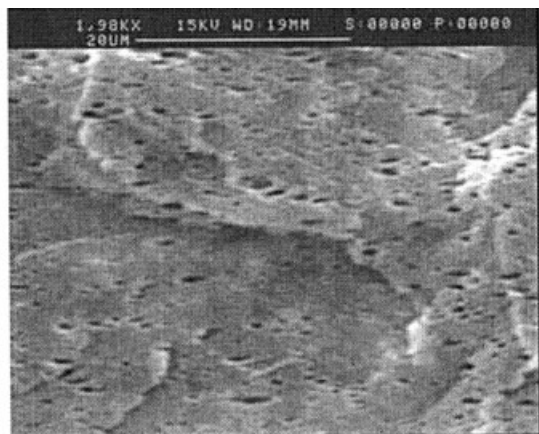
The storage modulus and loss modulus curves of the blends show that the values are between those of the pure component polymers. Figure 9 shows the temperature dependence $\tan \delta$ ($\tan \delta$) of ENR-50/EVA blends at different blend ratios. Pure ENR-50 shows a glass transition temperature (T_g) at -13.7°C

with a higher damping value. In the case of EVA, the T_g of EVA occurs at around -6°C . The peak intensity of the EVA phase is not so sharp because of the low damping value of this phase. For blends, a single transition occurs (T_g) which shifted toward the lower temperature region with blend ratio. This indicates that the two components (ENR-50 and EVA) are compatible at the amorphous region.

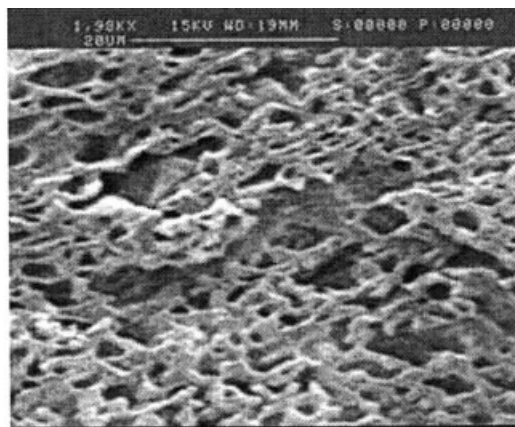
In many polymer blends and in the absence of any strong intermolecular interaction, the dissolved polymer act as a plasticizer, thus reducing the T_g of the resulting phase. In this kind of blend, usually negative deviations from the ideal (linear) T_g versus composition behavior occur. Moreover, the incorporation of the second component into the polymer matrix may affect chain packing, leading to low T_g values.¹⁹

According to Olagoke et al.²⁰ the appearance of one T_g is not a proof of miscibility but only a proof of a state of fine dispersion. The presence of a single or dual glass transition could depend on the particle size of dispersed phase in phase separated blends. SEM micrograph of tensile fractured surface of ENR-50/EVA blend at different blend ratios (Fig. 10) shows a fine dispersion of both components in the blend.

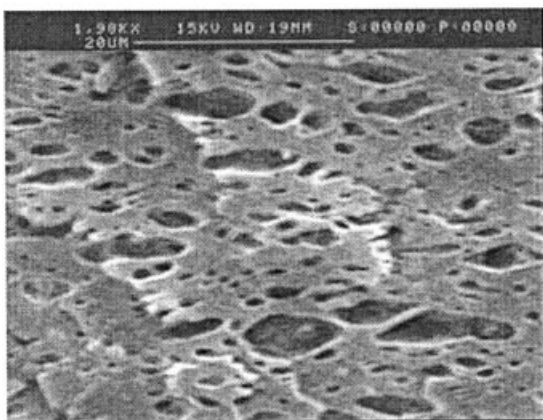
The temperature corresponding to the maximum in $\tan \delta$ peak and E'' is chosen as a T_g of the sample. As a general trend in polymer system, the T_g from $\tan \delta$ maximum is found to be higher than that of the E'' maximum. The individual T_g values from E'' maximum are found to be intermediate between those of



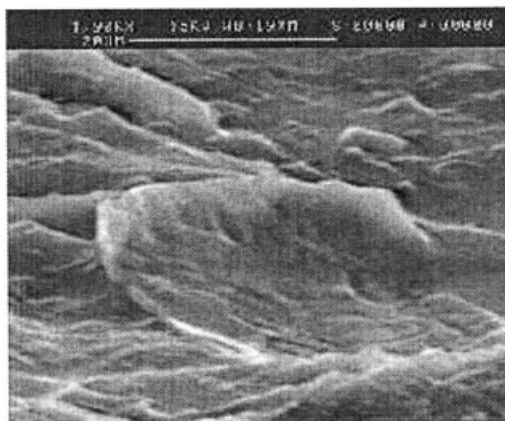
A)ENR-50 / EVA: 20 / 80



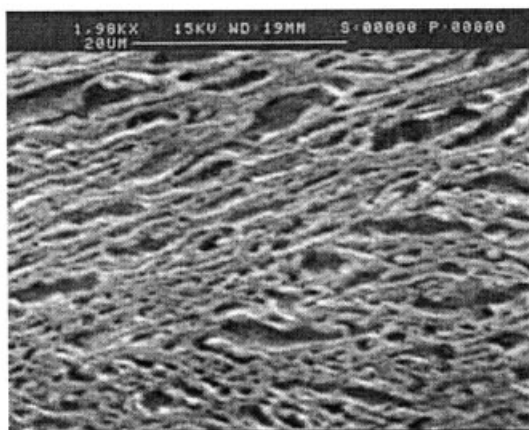
D)ENR-50 / EVA: 60 / 40



B)ENR-50 / EVA: 40 / 60



E)ENR-50 / EVA: 80 / 20



C)ENR-50 / EVA: 50 / 50

Figure 6 SEM micrograph of the surface of ENR-50/EVA blend at different blend ratios.

the individual components. This again indicates that the system is compatible at all ratios.²¹

The miscibility of the blend components can be predicted with dynamic mechanical data. Generally, for an immiscible blend, the $\tan \delta$ temperature curve shows the presence of two $\tan \delta$ damping peaks cor-

responding to T_g s of the individual polymer. For miscible blends, the curve shows a single peak between the transition temperatures of the component polymer.²² However, for a partially miscible system, a broadening of the transition occurs, and the T_g values are shifted to higher or lower temperatures as a func-

TABLE I
Dynamic Mechanical Properties and Density of ENR-50/EVA at Different Blends Ratios

Molar ratio of ENR-50/EVA	Damping max, Tan δ	T_g ($^{\circ}\text{C}$)		Density (g/cm^3)	
		Tan δ	E' peak	Measured	Calculated
0/100	0.262	-6	-30.36	0.93	0.93
20/80	0.393	-18.2	-24.58	0.94	0.95
40/60	0.532	-17.0	-22.55	0.95	0.97
50/50	0.652	-15.0	-21.61	0.96	0.98
60/40	0.781	-14.7	-21.88	0.97	0.99
80/20	1.199	-11.5	-20.89	1.00	1.01
100/0	1.945	-13.7	-22.43	1.02	1.03

tion of composition.¹⁶ In our case, blend of ENR-50/EVA are compatible since there is a single peak between the transition temperatures for all blend ratios.

Thermal analysis

Thermal gravimetric analysis

Thermograms and derivative thermograms of pure ENR-50, EVA, and their blends are shown in Figures 11 and 12, respectively. For pure EVA, degradation occurs in two stages. The first stage started at 315 $^{\circ}\text{C}$, leading to weight loss of 10%, and completed at 395 $^{\circ}\text{C}$. This stage involved acetic acid evolution and the second step involved main chain degradation, which started at 495 $^{\circ}\text{C}$ and completed at 514 $^{\circ}\text{C}$, with a weight loss of 90%. Pure ENR-50 started to de-

grade at 354 $^{\circ}\text{C}$ and completed at 479 $^{\circ}\text{C}$. Hence ENR-50 and EVA are stable up to 479 $^{\circ}\text{C}$ and 514 $^{\circ}\text{C}$, respectively.

Table II shows the data from TGA test. For polymer blends, the thermal degradation depends on the morphology and the extent of interaction between the phases.²³ It is interesting to note that initial degradation temperature (T_0), degradation temperature (T_{deg}), and final degradation temperature (T_{end}) of the blends are higher than that of individual components. T_{deg} corresponding to the main weight losses was obtained from derivative curves (DTG). Hence, it could be concluded that, blending of ENR-50 and EVA lead to the improvement in thermal stability and this might be due to some degree of interaction that has taken place among the blend materials. At 50:50 blend ratio of

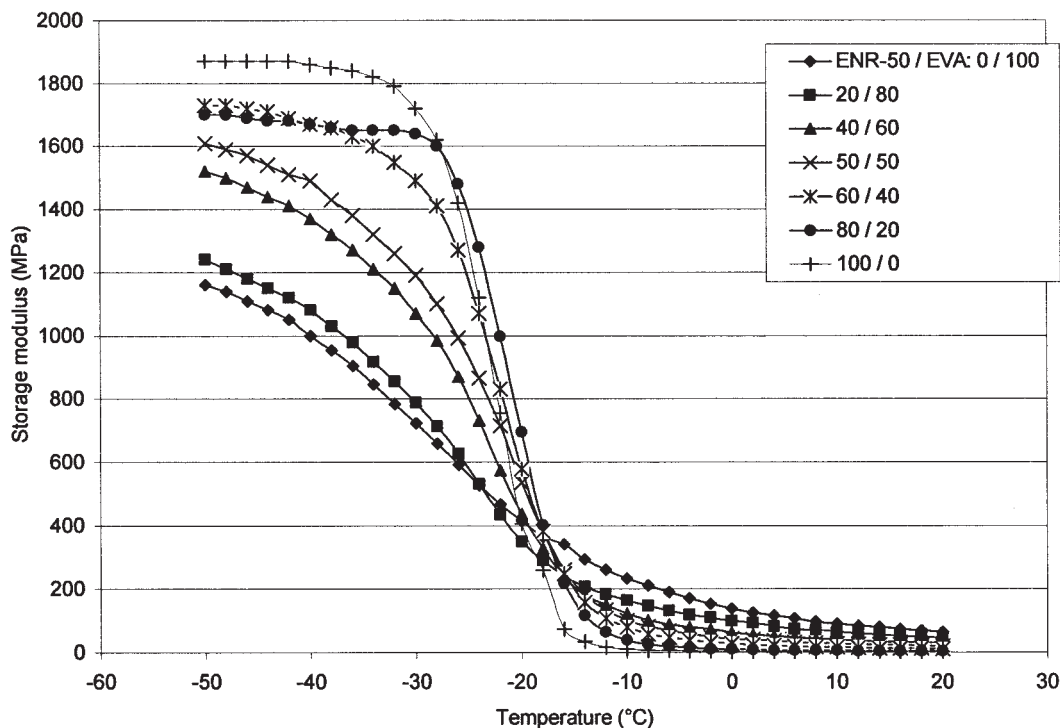


Figure 7 Storage modulus (E') versus temperature for ENR-50/EVA blend at different blend ratios.

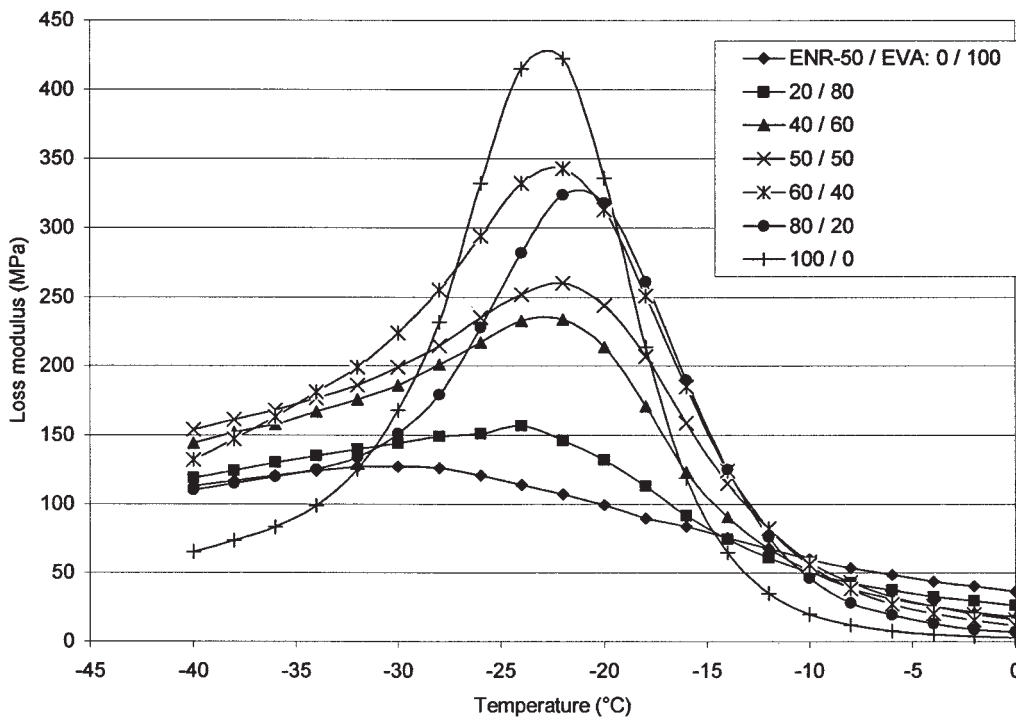


Figure 8 Loss modulus (E'') verses temperature for ENR-50/EVA blend at different blend ratios.

ENR-50/EVA, T_0 , T_{deg} , and T_{end} were registered at higher temperature when compared to other blend ratios and this indicates that, this blend ratio (50:50) is the most stable blend. In 50:50 blend ratios, both

ENR-50 and EVA are in continuous phase and produce a co-continuous morphology in the blend, as indicated in SEM study (Figure 6D). There was a drastic weight loss from 400 to 450°C for the blend

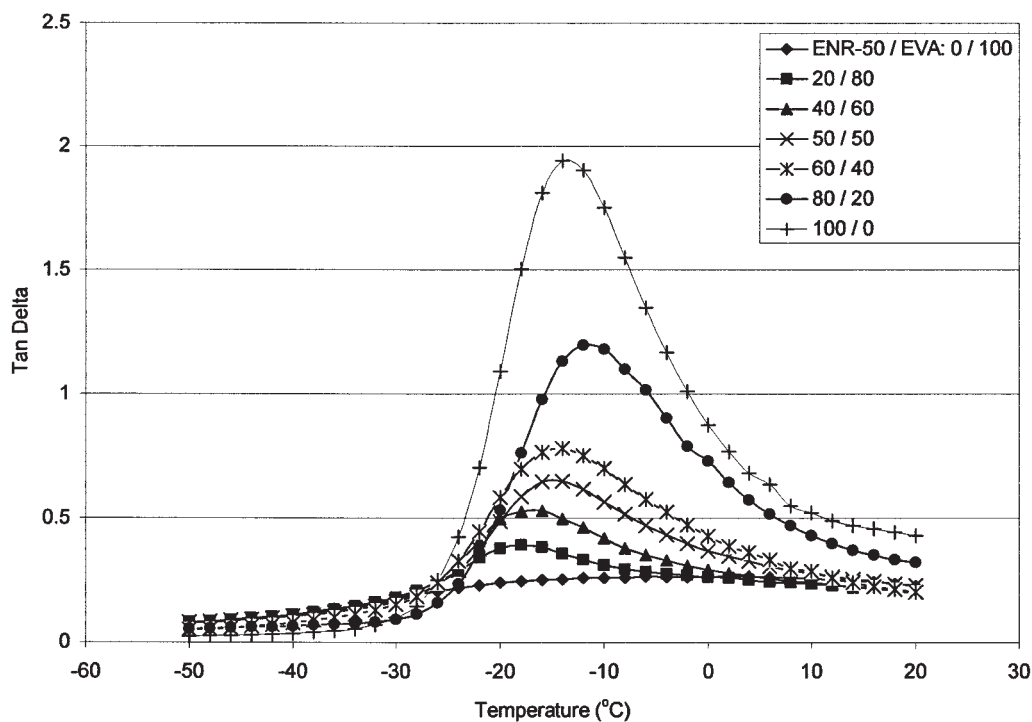
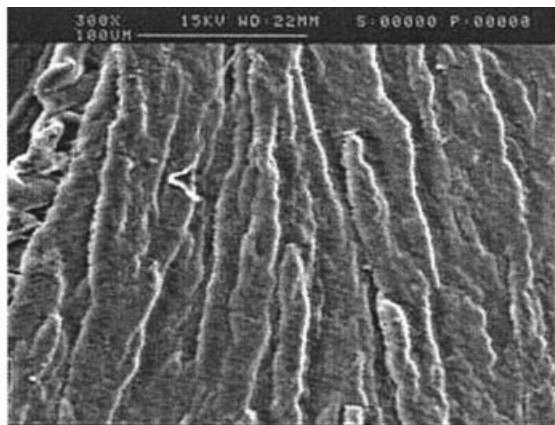
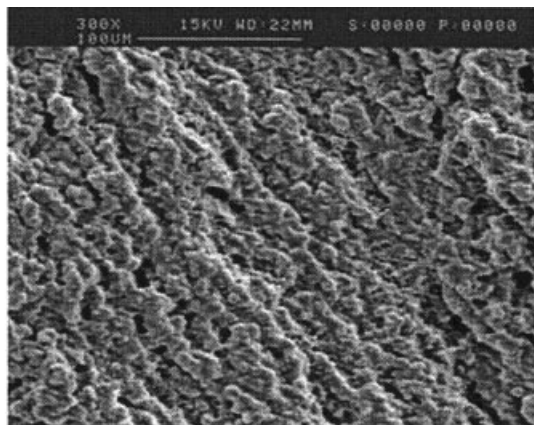


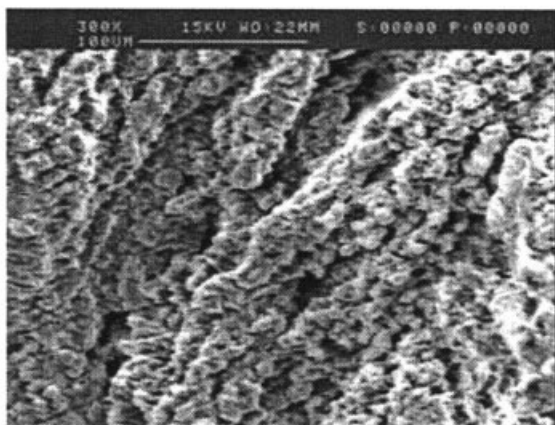
Figure 9 Tan delta ($Tan \delta$) verses temperature for ENR-50/EVA blend at different blend ratios.



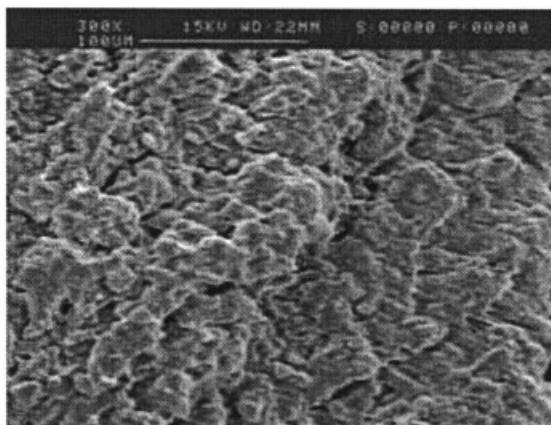
A)ENR-50 / EVA: 0 / 100



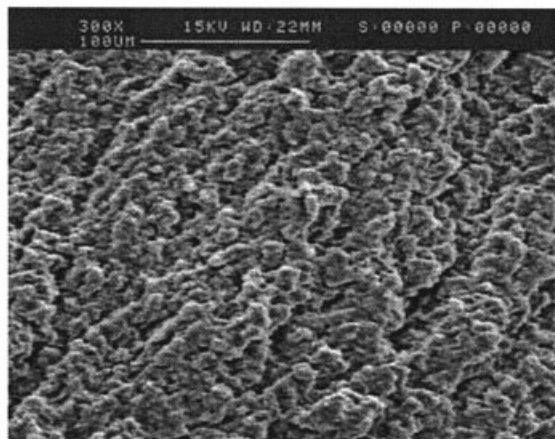
D)ENR-50 / EVA: 50 / 50



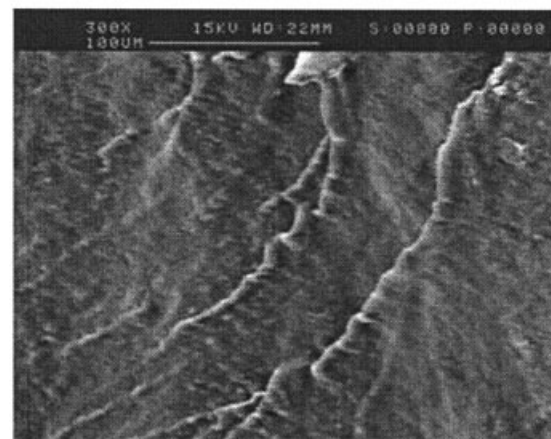
B)ENR-50 / EVA: 20 / 80



E)ENR-50 / EVA: 80 / 20



C)ENR-50 / EVA: 40 / 60



F)ENR-50 / EVA: 100 / 0

Figure 10 SEM micrograph of the tensile fractured surface of ENR-50/EVA blend at different blend ratios.

with 50 wt % and above ENR-50. It could be concluded that at these temperature, increase in ENR-50 content leads to decrease in thermal stability of the blend.

Differential scanning calorimetry analysis

Differential scanning calorimetry (DSC) measurement was performed to characterize the crystallization and

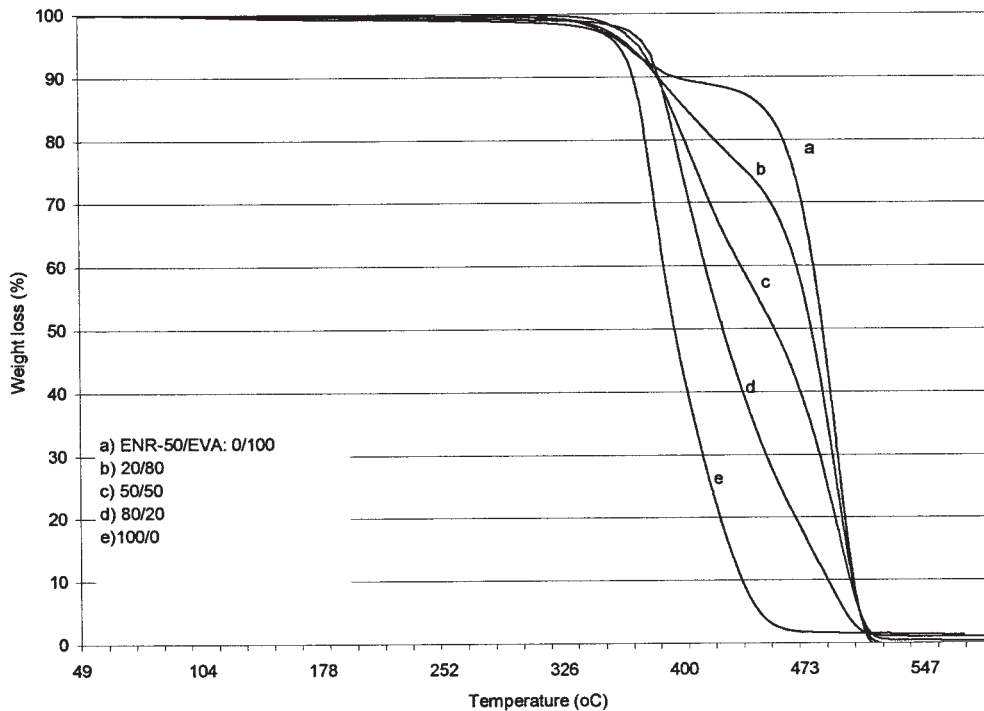


Figure 11 Thermograms of ENR-50/EVA blend at different blend ratios.

melting behavior of ENR-50/EVA blends. DSC results for ENR-50/EVA blends at different blend ratios are compared in Table III and Figure 13. The area of the melting endotherm was reported as the heat of fusion

(ΔH_f). The blends displayed a two-peak point temperature, whose maximum value was taken as the melting point (T_m). Marcilla et al.²⁴ reported similar DSC curve for pure EVA.

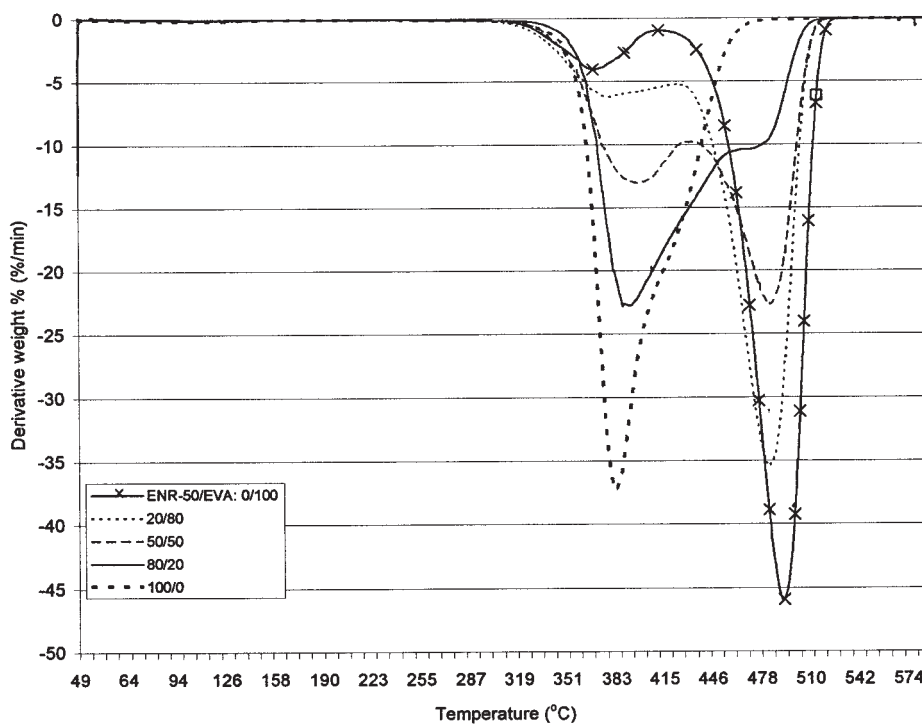


Figure 12 Derivative thermograms of ENR-50/EVA blend at different blend ratios.

TABLE II
Degradation Temperature and Weight Loss of ENR-50/EVA Blends at Different Blend Ratios

Blend ratio of ENR-50/EVA	T_0 (°C)	T_{deg} (°C)	T_{end} (°C)	Total weight loss (%)	Weight loss (%) at	
					400°C	450°C
0/100	315,495	369,494	395,514	100	10.37	14.89
20/80	330	388,493	518	99.14	14.29	28.2
50/50	343	406,494	522	98.35	18.91	46.92
80/20	322	403,483	517	98.68	23.92	69.23
100/0	287	402	479	98.44	27.1	87.67

From Table III it can be seen that ΔH_f values decrease with the increase in ENR-50 content in the blends. The heat of fusion values depend on the crystallinity of the material. Hence, the crystallinity of these blends can be calculated and predicted from ΔH_f values as the ratio of ΔH_f of the blend and ΔH_f of pure EVA ($\Delta H_f = 41.05$ J/g). The percentage of crystallinity in the blends decreases with increase in the ENR-50 content. George et al.²³ reported that the decrease in ΔH_f values and crystallinity

is due to the fact that the formation of crystallite in the blend was effected by the presence of rubber phase. Koshy et al.²⁵ found that the crystallinity of the blends decrease with increase in the addition of natural rubber (NR), indicating the migration of NR phase into the interchain space of EVA.

The melting temperature (T_m) corresponding to the melting endotherm also reduces upon incorporation of ENR-50 to EVA. This might be due to the noncrystallisable component that retards the crystal growth, which lead to imperfect crystal as discussed earlier. However, there is no significant difference in T_m when the amount of ENR-50 content in the blend increased. This observation indicated that there was no effect of blend ratio toward the T_m of the system.

TABLE III
Melting Characteristic and Crystallinity of ENR-50/EVA Blends at Different Blend Ratios

Molar ratio of ENR-50/EVA	T_{onset} (°C)	T_m (°C)	ΔH_f (J/g)	Crystallinity (%)
0/100	53.6	88.04	41.05	100
20/80	53.5	86.87	35.35	86.1
50/50	53.87	86.66	16.90	41.2
80/20	53.88	86.01	5.65	13.8

CONCLUSIONS

On the basis of the above results and discussion, the following statements can be drawn:

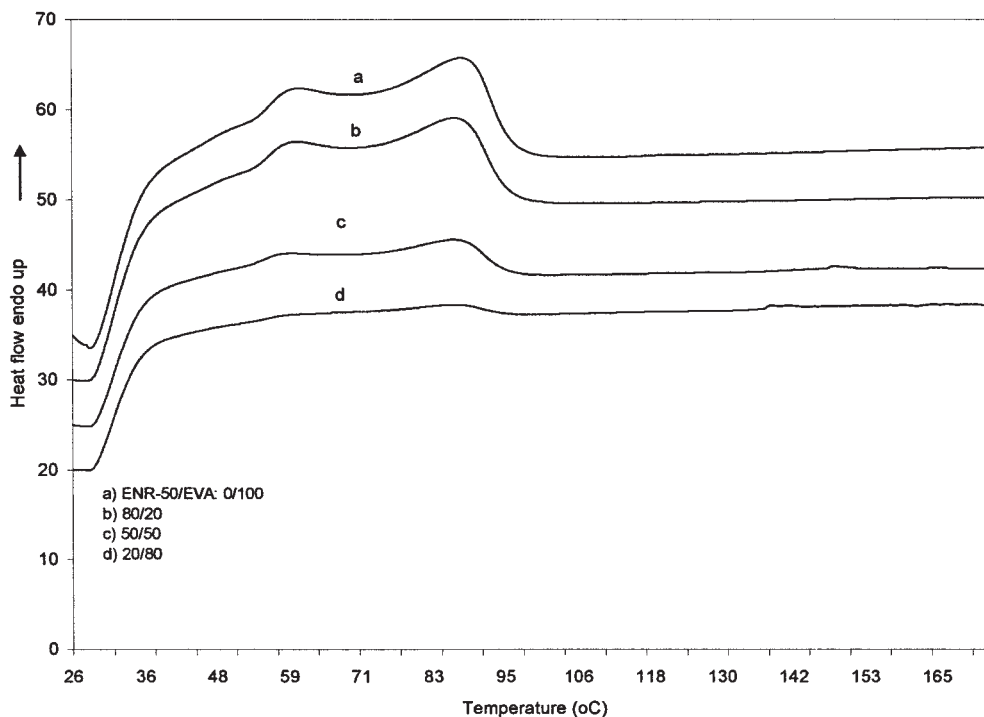


Figure 13 Differential scanning calorimetric curves of ENR-50/EVA blend at different blend ratios.

1. The tensile properties of the ENR-50/EVA blend increase with the increase of EVA content.
2. In the ENR-50/EVA blends at 20:80 and 40:60 blend ratios, the minor phases exist as a dispersed phase in a major continuous phases, whereas in 50:50, 60:40, and 80:20 blend ratios, both the phases exist as continuous phases, producing a co-continuous morphology.
3. The dynamic mechanical properties proved that the blends are compatible.
4. The thermal stability results proved that the blending of ENR-50 and EVA leads to the improvement in thermal stability and 50:50 blend ratios is the most stable blend.

References

1. Ismail, H.; Suzaimah, S. *Polym Test* 2000, 19, 879.
2. Poh, B. T.; Ismail, H.; Quah, E. H. *Polym Test* 2001, 20, 389.
3. Hao, P. T.; Ismail, H.; Hashim, A. S. *Polym Test* 2001, 20, 539.
4. Alex, S.; Sirqueira, Soares, B. G. *Eur Polym J.* 2003, 39, 2283.
5. Varghese, H.; Bhagawan, S. S.; Rao, S. S.; Thomas, S. *Eur Polym J* 1995, 31, 457.
6. Jasen, P.; Gomes, A. S.; Sores, B. G. *J Appl Polym Sci* 1996, 61, 591.
7. Ismail, H.; Supri; Yusof, A. M. M. *Polym Test* 2004, 23, 675.
8. Chowdhury, S. R.; Mishra, J. K.; Das, C. K. *Polym Degrad Stab* 2000, 70, 199.
9. John, B.; Varughese, K. T.; Ommem, Z.; Potschke, P.; Thomas, S. *J Appl Polym Sci* 2003, 87, 2083.
10. Halimatudahliana; Ismail, H.; Nasir, M. *Polym Test* 2002, 21, 163.
11. Chen, X.; Zhong, H.; Jia, L.; Tang, R.; Qiao, J.; Zhang, Z. *Int J Adhesion Adhesives* 2001, 21, 221.
12. Li, C.; Kong, Q.; Zhao, J.; Zhao, D.; Fan, Q.; Xia, Y. *Mater Lett* 2004, 58, 3613.
13. Gelling, I. R. *J Nat Rubber Res* 1991, 6, 184.
14. Baker, C. S. L.; Gelling, I. R. In *Epoxidise Natural Rubber in Development in Rubber Technology-4*; Whelan, A., Lee, K. S., Eds.; Elsevier Applied Science: London, 1987.
15. Kallitsis, J. K.; Kalfoglou, N. K. *J Appl Polym Sci* 1989, 37, 453.
16. Doak, K. W. Ethylene Polymer. In *Encyclopedia of Polymer Science and Engineering*, Mark, H. F., Bikales, N. M., Overberger, C. G., Menges, G., Eds.; Wiley: New York, 1986; Vol. 6.
17. Ismail, H.; Mohamad, Z.; Bakar, A. A. *Polym Plast Tech Eng* 2003, 4, 81.
18. Soares, B. G.; Alves, F. F.; Oliveira, M. G.; Moreire, A. C. F.; Garcia, F.G.; Lopes, M. F. S. *Eur Polym J* 2001, 37, 1577.
19. Bikiaris, D.; Prinios, J.; Botev, M.; Betchev, C.; Panayiotou, C. *J Appl Polym Sci* 2004, 93, 726.
20. Olagoke, O.; Robeson, L. M.; Shaw, M. T. *Polymer-Polymer Miscibility*; Academic Press: New York, 1979.
21. Varughese, K. T.; De, P. P. *J Appl Polym Sci* 1989, 37, 2537.
22. Utraki, L. A. *Polymer Alloys and Blend*; Hanser: New York, 1989.
23. George, S.; Varughese, K. T.; Thomas, S. *Polymer* 2000, 41, 5485.
24. Marcilla, A.; Sempere, F. J.; Reyes-Labarta, J. A. *Polymer* 2004, 45, 4977.
25. Koshy, A. T.; Kuriakose, B.; Thomas, S.; Varghese, S. *Polymer* 1993, 34, 2438.